PERGAMON

Chaos, Solitons and Fractals 11 (2000) 1835–1848

CHAOS
SOLITONS & FRACTALS

www.elsevier.nl/locate/chaos

Effect of noise on the tuning properties of excitable systems

André Longtin *

Département de Physique, Université d'Ottawa, 150 Louis Pasteur, Ottawa, Ontario, Canada K1N 6N5

Abstract

We analyze the effect of additive dynamical noise on simple phase-locking patterns in the Fitzhugh–Nagumo (FHN) two-dimensional system in the excitable regime. In the absence of noise, the response amplitude for this system displays a classical resonance as a function of driving frequency. This translates into V-shaped tuning curves, which represent the amplitude threshold for one firing per cycle as a function of forcing frequency. We show that noise opens up these tuning curves at mid-to-low frequencies. We explain this numerical result analytically using a heuristic form for the firing rate that incorporates the frequency dependence of the subthreshold voltage response. We also present stochastic phase-locking curves in the noise intensity-forcing period subspace of parameter space. The relevance of our findings for the tuning of electroreceptors of weakly electric fish and their encoding of amplitude modulations of high frequency carriers are briefly discussed. Our study shows that, in certain contexts, it is essential to take into account the frequency sensitivity of neural responses and their modification by sources of noise.

1. Introduction

Tuning curves are an important characteristic of excitable systems such as neurons and cardiac cells. They describe the sensitivity of these cells to the amplitude and frequency of periodic signals (see [1–3] and references therein). Such cells are also driven by noise sources, such as intrinsic conductance fluctuations, synaptic input, or external environmental or stimulus fluctuations. The presence of these sources can significantly alter the firing pattern of any periodically driven cell. For a periodically driven pacemaker, noise can make the firing patterns highly irregular, and blur the transition between different phase-locked behaviors as parameters are varied [4]. If instead the cell is excitable, as is of interest here and in many biological systems, noise induces firings even without periodic drive. And as intrinsic or external noise levels vary, the threshold amplitude for firing may be altered. Hence, noise makes the notion of a tuning curve somewhat ambiguous. It is therefore of great interest to entangle the tuning properties of the cell shaped by the deterministic components of transduction and firing processes from those shaped by stochastic components.

Our work is motivated by recent findings [2] that mechanoreceptor tuning curves can be significantly altered by externally added stimulus noise. It is also motivated by ongoing research into the mechanisms underlying aperiodic phase-locked firing in many excitable neurons, where noise produces mildly perturbed n:m patterns (n stimuli eliciting m firings) for large stimulus amplitudes, and allows small subthreshold stimuli to be expressed. Further motivation comes from work in the area of stochastic resonance (SR), in particular from its application to biological systems [5–7] (see [8] for a review).

There has been a variety of studies of SR applied to neuronal systems. The regime often encountered is that where the neuron acts as a simple thresholding system, firing a spike whenever the voltage reaches

* Tel.: +613-562-5800 ext. 6762; fax: 613-562-5190.
E-mail address: andre@physics.uottawa.ca (A. Longtin).

0960-0779/00/$ - see front matter
PII: S0960-0779(99)00120-4

threshold. Simplified models based on modulated point processes [9], crossing statistics of a static threshold [10], or one-dimensional versions [11] of the Fitzhugh–Nagumo system (FHN) system considered in this paper can explain some of the properties of neurons driven by slow signals. They do not however take into account the possible frequency dependence of the response of the cells, nor the refractory properties that come into play for higher frequency signals and/or high firing rates that occur at high noise intensities. In a sensory receptor, the frequency dependence may arise from the processes at the spike initiation zone of the neuron which connects to a receptor, as well as from filtering due to specialized structures in the receptor, such as those of the cochlea [1]. For example, certain mechanoreceptors respond preferentially to low frequency signals, while others neglect such signals and respond only to high frequency ones (see e.g. [2,3]).

When signal frequencies are commensurate with or faster than internal neuron time scales, the noise intensity that optimizes firing statistics such as the spectral amplification becomes frequency-dependent [8,12]. Also, the basic frequency dependence of the threshold for firing e.g. one spike per forcing cycle determines the shape of the tuning curves of the cells. This tuning curve is not analytically calculable for deterministic nonlinear neuron models such as the FHN considered in this paper. Thus, it is not surprising that they have not been studied in any analytical detail when both stochastic and deterministic forcing are present. We note that there has been one numerical study which reported that noise modifies the tuning curves of the FHN sytem used as a model of the acoustic nerve [13].

The present study explores this effect of noise on tuning properties in greater detail. It proposes a heuristic approach to the study of noisy tuning curves. It is based on a modified Kramers rate in which the frequency dependence of the subthreshold voltage amplitude is approximated. The basic idea is that the complex two-dimensional barrier crossing problem for the simple yet realistic FHN model is replaced by a one-dimensional barrier crossing problem in which there are an effective amplitude and an effective potential that depend on frequency and noise. The approach can be used to approximate the tuning properties of real neurons. We show that noise can have a drastic effect on the shape of tuning curves.

The paper is organized as follows. In Section 2, we present the FHN model used for our study of noisy tuning curves, and discuss its numerical integration and deterministic properties. Section 3 considers the phase-locking curves for 1:1 firing in the forcing amplitude-forcing period subspace for different noise levels. Section 4 presents a heuristic theory for the stochastic tuning curves (STCs) which combines Kramers escape rate theory with the frequency dependence of the subthreshold response. Section 5 discusses another heuristic approach to the STCs based on the frequency dependence of an "effective potential for firing". Section 6 summarizes recent findings on stochastic phase locking viewed from the noise intensity-forcing period subspace, and its relevance to SR studies. Section 7 discusses the relevance of our findings to biological receptors, and in particular to electroreceptors. The paper ends with a discussion in Section 8.

2. Model and methods

Our approach involves analyzing how additive noise alters the stimulus amplitude-period combinations that produce simple deterministic phase locking patterns in a model excitable cell [14,15]. We also show how this noise induces average locking patterns in the subthreshold regime, and alters the threshold amplitude for given deterministic patterns. The Fitzhugh–Nagumo neuron model with sinusoidal forcing and additive noise was chosen [13,16]:

$$\dot{v} = v(v - 0.5)(1 - v) - w + A\sin\beta t + I + \eta(t), \tag{1}$$

$$\dot{w} = v - w - b, \tag{2}$$

$$\dot{\eta} = -\lambda\eta + \lambda\xi(t). \tag{3}$$

Here v is the voltage variable, w the recovery variable, and $\xi(t)$ a zero-mean Gaussian white noise of intensity D, which is lowpass-filtered to produce the exponentially correlated noise η (correlation time $t_c = \lambda^{-1}$). The noise η is coupled additively to v. Parameters are $I = 0.04,\ b = 0.15,\ \epsilon = 0.005,\ t_c = 10^{-3}$ (quasi-white noise); the firing threshold is 0.5, and a firing is counted only if separated from a previous one by at least the absolute refractory period $T_R = 0.4$ s (in the time units of the model; this corresponds to e.g., 1 ms in real time).

Numerical integration of this stochastic model uses the Manella–Palleschi 3/2-order algorithm with an integration time step of 0.001 for $T < 1$ and 0.0025 otherwise. The noise is meant to represent either conductance fluctuations or synaptic noise. As the FHN system is a reduced description of a conductance-based model, its parameters do not have straightforward biophysical interpretations; nevertheless, the lumped effect of different noise sources can, to a first approximation, be studied via the additive dynamical noise used in Eq. (3) (see also [17] and references therein).

In the absence of noise, the tuning curve for a given n:m phase-locked pattern (m spikes during n cycles) is obtained by finding, for each T, the minimum amplitude A which elicits that pattern. Stochastic tuning curves (STCs), i.e., tuning curves for $D > 0$, are more difficult to compute numerically. We use a search algorithm which evaluates mean $n : m$ phase-locking ratios using 100 stimulus-cycle realizations of the stochastic process Eqs. (1)–(3). For each period $T = 2\pi/\beta$, the algorithm closes in on the amplitude A giving the desired mean ratio (for example, which gives a ratio close to one, i.e., one spike per period on average). A given search converges on the amplitude value using realizations over smaller and smaller amplitude ranges. Due to statistical fluctuations in the mean firing rate across realizations, a search is more likely to be successful if the desired accuracy to which the amplitude is determined is not too high, and the noise not too strong. Thus, the amplitude value actually plotted is an average of the values obtained from three *successful* searches using different realizations.

3. Forcing amplitude–period subspace

Without noise, the minimum forcing amplitude A in Eq. (1) which produces a given number of spikes per forcing cycle depends strongly on the forcing period T. This is illustrated in Fig. 1(a) and (b), where the bold symbols are used to represent the minimum amplitude to observe 1:1 and 2:1 firing. Such firing patterns are periodic. The 2:1 pattern, and in fact all $n : m$ firing patterns with $n, m > 1$, are found over smaller regions of parameter space compared to the 1:1 pattern. Also, each pattern has a best period, i.e., a period for which the minimum required amplitude is itself a minimum (e.g. $T \approx 1.3$ for 1:1).

We note that the existence of a best period, and indeed of a V-shaped tuning curve for $D = 0$, is intimately related to the fact that the FHN system has a resonance (see Fig. 6(a)) at a frequency close to the imaginary part of the eigenvalues of the FHN flow linearized around its fixed point.

We next compute the amplitude-period phase-locking curves with noises of different intensities. The results are shown in Fig. 1 alongside those for the noiseless case. It is important to remark at the outset that, when $D > 0$, the firing patterns are not strictly periodic, even though the firings tend to occur over a small range of phases (see Figs. 2 and 3). Phase-locking ratios are hence defined as average ratios [4]. For example, a 1:1 pattern for a given $D > 0$ may have a cycle with two or more spikes, and others with none at all, yet on average there is one spike per cycle.

Fig. 1 shows that the tuning curves change shape when noise is present, as observed in [13]. At higher frequencies and larger amplitudes, there exist regions of parameter space that produce the same locking ratio, just like for deterministic oscillators [15]. The 1:1 curves there are a lower boundary of the 1:1 region. Outside this subregion of parameter space, the locking ratios vary continuously as a function of forcing parameters. Noise then allows a smooth transition between phase-locking ratios, which no longer are limited to ratios of integer (i.e., to rational numbers).

At mid-to-low frequencies (mid-to-high periods), where the midpoint refers to the best frequency (best period), the curves are pulled down into the deterministically silent region. At higher frequencies the curves are not altered much by noise. For periods less than the best period, the threshold for 1:1 increases slightly with D. At high noise the STC may even become monotonic. The best period for $D = 0$ and for low D is then no longer the best. Hence, increasing D opens up the V-shaped 1:1 tongue at mid-to-high periods, converting it to an L-shaped tongue, all the while leaving the threshold almost unchanged at low periods. Noise thus increases the bandwidth at longer periods. Such results have been recently observed in experimental preparations involving neurons which slowly adapt to mechanical vibrations [2].

The basic behavior of these tuning curves can be understood from Figs. 2 and 3, which show membrane voltage time series for different combinations of A and D. The deterministic cases correspond to periodic 1:1 patterns with precise phase-locking. For $T = 10$, the amplitude must be lowered from that which yields 1:1

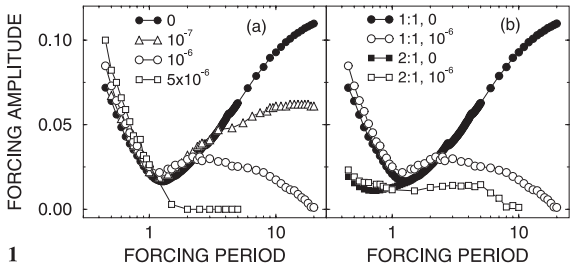

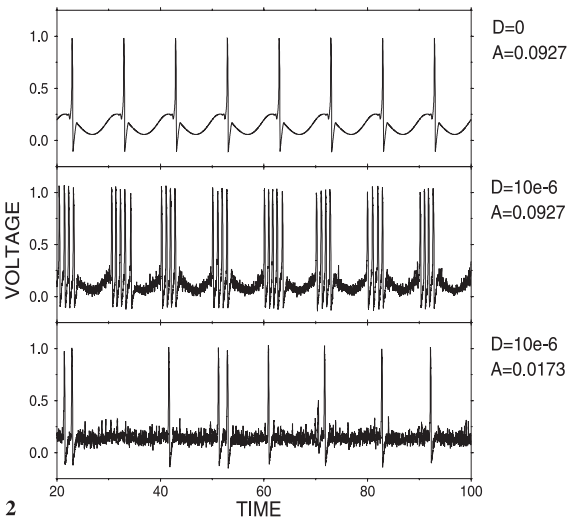

Fig. 1. Stimulus amplitude–period pairs for which the numerical integration of Eqs. (1)–(3) yields (a) one firing per sinusoidal forcing cycle on average, and (b) one firing every two cycles on average. The 1:1 results from (a) for the noise intensities $D = 0$ and $D = 10^{-6}$ are reproduced in (b) for comparison. The legend in (a) indicates the value of D for each curve; the one in (b) further indicates the average locking pattern. Solid symbols denote the minimal amplitude (i.e., the "threshold") for 1:1 and 2:1 firing when $D = 0$ in Eq. (3), i.e., for deterministic periodic 1:1 and 2:1 firing patterns. The deterministic subthreshold region is bounded from above by this 1:1 curve for $T > 1.5$, and by the 2:1 curve for $0.8 < T < 1.5$.

Fig. 2. Membrane voltage time series obtained from numerical integration of Eqs. (1)–(3) with a long forcing period ($T = 10$). Noise intensity D and forcing amplitude A are indicated beside each panel. The top panel is for $D = 0$ and the minimal A that produces one firing per cycle. The middle panel corresponds to the same A but with $D > 0$. The bottom panel has the same D as the middle panel, but a decreased A in order to obtain 1:1 firing on average.

firing when $D = 0$ in order to get 1:1 on average. For $T = 1$, the opposite holds, as the amplitude must now be increased to counteract the deletion of spikes by the noise. The relatively invariant shape of the curves at low T is due in particular to the absolute refractory period, which cannot be overcome by noise.

For larger D, such as for $D = 5 \times 10^{-6}$, the tongue reaches zero, e.g. at $T \approx 1.5$ for the mean 1:1 pattern. This implies that for $T \approx 1.5$, noise alone (i.e., even for $A = 0$) is sufficient to produce a mean locking ratio of one; and for $T > 1.5$, noise alone produces a larger than desired ratio. The same is seen for the 1:1 pattern at $T \approx 20$ when $D = 10^{-6}$. Fig. 1(b) shows the same effect for the 2:1 pattern with $D = 10^{-6}$, the 2:1 curve joins the deterministic one at lower T, but opens up and eventually reaches the T-axis at $T \approx 10$. Our theory below predicts these values of T where the STCs reach the T-axis.

4. Heuristic theory of STCs

4.1. The flat adiabatic response case

In this section, we present a heuristic analysis of stochastic tuning curves using a Kramers-type approach. Such an approach has been used for model neurons driven by noise and periodic forcing [9,11,18]. In [11], an expression for the firing rate was derived for the FHN model studied here. It is a function mainly of D, the distance between the resting potential and the threshold, and the forcing amplitude A, and was derived in the adiabatic limit where signals evolve on a time scale slower than all neuron time scales. This allows the use of a one-dimensional reduced FHN system, in which the slow variable w instantaneously relaxes to its equilibrium value.

While this and other adiabatic approaches are useful for studying e.g. the correlation between slow driving signals and the firing rate [6,11], it must be extended to study tuning properties, since by definition that approach assumes all frequencies are slow and have the same effect on the firing. A one-dimensional FHN model is by definition overdamped and thus cannot have the complex eigenvalues necessary for a

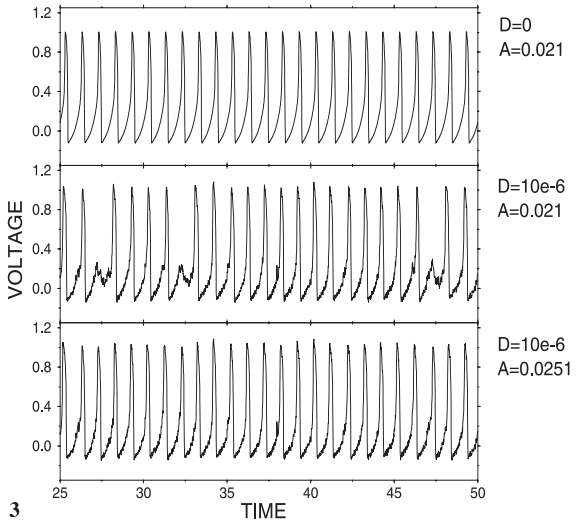

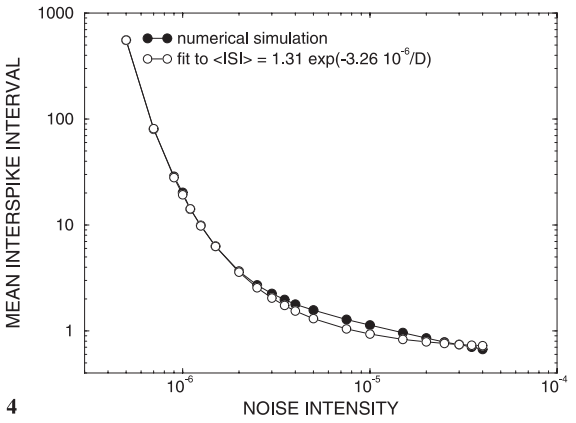

Fig. 3. Membrane voltage time series as in Fig. 2, but for a shorter forcing period ($T = 1$). In contrast to Fig. 2, the amplitude here has to be slightly increased to obtain 1:1 firing on average in the presence of noise (bottom panel), since the noise deletes firings from the deterministic 1:1 pattern (middle panel).

Fig. 4. Numerically computed mean interspike interval versus the noise intensity D for Eq. (3) in the absence of sinusoidal forcing. The exponential fit is very satisfactory for $D < 3 \times 10^{-6}$, but begins to deviate from this behavior for larger D. The fitted values are given in the inset.

deterministic resonance. Rather, the low-amplitude frequency response of such a system has a lowpass characteristic, which is relatively flat at low frequencies. The response function of the actual two-dimensional FHN dynamics is not of low-pass type, but is bell-shaped (see Fig. 6(a)), as is typical for oscillators, and in particular for subthreshold oscillators such as excitable systems. Further, recent work has shown that faster signals will also interact with the recovery process [12].

Our first approach to understand the STC shapes is to consider a modified Kramers rate in which the amplitude of the forcing is frequency-independent. We study the resulting "baseline" STCs for such a "flat frequency response". We then make an ansatz for the form of the frequency dependence, and show that the resulting STCs are similar to those in Fig. 1.

In the absence of periodic modulation ($A = 0$), the firing rate can be written in the standard form $R_0 = f(\mu)$, where $\mu = U_0/D$ is a dimensionless parameter corresponding to the ratio of the potential barrier to D (see e.g., [8]). U_0 can be considered as the distance from fixed point to the threshold for firing. This of course is a rough approximation since the FHN system is not a potential system. When U_0/D is large, one can use an Arrhenius-type expression for this rate: $R_0 = C\exp(-U_0/D)$. This is justified by the reasonably good fit of this expression to the data shown in Fig. 4, which plots the mean interspike interval versus D. For higher D, the behavior is better fitted by a power law. A more thorough analysis of spontaneous firing in this model can be found in [18]. The main simplification here is that the distance between the voltage and the threshold is dependent only upon one variable, the voltage itself. In other words, we are neglecting the fact that the threshold is really a curve that goes though the two-dimensional v–w plane in this one-dimensional reduced FHN model.

We refer to the rate as a Kramers rate, even though we do not write the prefactor explicitely in terms of the curvatures around the fixed point and barrier maximum. For $A > 0$ in Eq. (1), we can write a modified time-dependent Kramers rate $R(t)$ [8]

$$R(t) = f(\mu + \eta_0 \cos \omega t) = C\exp(-U_0/D)\exp(-\gamma\tilde{A}\cos(\omega t)/D), \tag{4}$$

where $\eta_0 = \gamma\tilde{A}/D$. The quantity $\gamma\tilde{A}$ has the same units as D, namely mV^2/s (the membrane potential is in mV, although scaled units are used in this version of FHN). We consider $\tilde{A}$ to be an effective amplitude of the steady-state voltage oscillation $v(t)$ in response to the amplitude A of the forcing term in Eq. (1).

Loosely speaking, it measures the effectiveness of $v(t)$ to trigger spikes. While $\tilde{A}$ is proportional to A, the proportionality constant depends on A, T and D, as we will see below. γ is a parameter describing an effective one-dimensional potential *in the presence of sinusoidal periodic forcing*. It may be a function of T and D as well as of the intrinsic parameters of the unforced FHN model.

The average phase-locking condition corresponding to a firing pattern with m spikes per n forcing cycles, each cycle having duration T, can then be written

$$\overline{R(t)} = \frac{1}{T}\int_0^T C\exp(-U_0/D)\exp(-\gamma\tilde{A}\cos(\omega t')/D)\,\mathrm{d}t' = \theta_{n,m}/T, \tag{5}$$

where $\theta_{n,m} = m/n$ determines the particular phase-locking pattern of interest. We are concerned in this paper only with average 1:1 and 2:1 patterns, for which we have $\theta_{1,1} = 1$ and $\theta_{2,1} = 0.5$. The average locking condition becomes

$$R_0 I_0(\gamma\tilde{A}/D) = \theta_{n,m}/T, \tag{6}$$

where I_0 is a modified Bessel function of order zero. If γ is a constant, then for each T and a given D, the condition Eq. (6) determines a value for $\tilde{A}(T,D)$. In the next section, we correct the resulting $\tilde{A}(T,D)$ curves for the subthreshold response properties of the FHN model.

So for now, we assume that γ is constant; the qualitative shape of the curves will not depend on this constant, as long as $\gamma > 0$. For simplicity, we choose $\gamma = -U_0$, where U_0 is obtained from the fit in Fig. 4. The values of $\tilde{A}(T,D)$ that satisfy Eq. (6) are determined numerically for each T using Newton's root finding method. The resulting "tuning" curves are shown in Fig. 5 for three values of D. Some similarity to the behavior of the curves in Fig. 1(a) is seen. For increasing D, one clearly sees a progression from horizontal tuning curves to curves that join the T-axis with a very negative slope. Fig. 5 indeed shows that the dependence of this 1:1 threshold amplitude on T is very weak for $T = 10^{-7}$, and becomes very pronounced for $D = 5\times10^{-6}$. However, the resulting curves do not have the preferred frequencies as in Fig. 1 and in many real neurons, and so the term "tuning curves" may not be the most appropriate. But the source of the "preferred frequencies" is not yet present in this simple model, and must be added subsequently.

Our flat response analysis can be pushed further to explain certain qualitative features of these tuning curves. We first consider their behavior as $D \to 0$. We show that for vanishing D, $\partial\tilde{A}/\partial T \to 0^-$, which is almost the case for $D = 10^{-7}$ in Fig. 5. For small D, the argument of I_0 is large, and we can use its asymptotic expansion $I_0(\gamma\tilde{A}/D) \sim \exp(\gamma\tilde{A}/D)/\sqrt{\gamma\tilde{A}/D}$. Assuming that for a given curve, D, U_0, γ and $\theta_{n,m}$ are fixed, we can consider for now that $\tilde{A} = \tilde{A}(T)$. Deriving each side of Eq. (6), we find

$$-\frac{\theta_{n,m}}{T^2} = C\exp(-U_0/D)\exp(\gamma\tilde{A}/D)\frac{\partial\tilde{A}}{\partial T}\left(-\frac{1}{2\tilde{A}}+\frac{\gamma}{D}\right)\left(\gamma\tilde{A}/D\right)^{-1/2} = \frac{\theta_{n,m}}{T}\left(\frac{\gamma}{D}-\frac{1}{2\tilde{A}}\right)\frac{\partial\tilde{A}}{\partial T}. \tag{7}$$

From this we can isolate

$$\frac{\partial\tilde{A}}{\partial T} = \frac{1}{(1/2\tilde{A}-\gamma/D)T}, \tag{8}$$

which indeed tends to 0^- provided $\gamma\tilde{A}/D > 0.5$. This restriction is consistent with our initial hypothesis that D is small, which allowed us to use the asymptotic expansion for I_0. Hence, the flat response STCs are horizontal for vanishing D.

It is also interesting to note that, for small D, we can write

$$\frac{\theta_{n,m}}{T} = C\exp\left[(-U_0+\gamma\tilde{A})/D\right]D^{1/2}/(\gamma\tilde{A})^{1/2}. \tag{9}$$

As $D \to 0$, the right-hand side goes to zero for $(-U_0+\gamma\tilde{A}) < 0$, and thus the only way the average locking condition Eq. (6) can be satisfied is by focussing on smaller values of $\theta_{n,m}$, i.e., on patterns that have fewer and fewer spikes per cycle.

We now show that Eq. (6) cannot be fulfilled when D is too large. In other words, if D is too large, the mean firing rate with noise alone (i.e., $\tilde{A} = 0$) may already be equal or greater than the value $\theta_{n,m}/T$. A Taylor expansion of I_0 now yields

$$\tilde{A} = \frac{2D}{\gamma}\left(\frac{\theta_{n,m}}{TR_0} - 1\right)^{1/2}. \tag{10}$$

From this, it is clear that for $\tilde{A}$ to be real, the condition $\theta_{n,m}/T > R_0$ must hold. This means that the spontaneous rate (with $\tilde{A} = 0$) must be less than the rate associated with the desired average locking condition, $\theta_{n,m}/T$. When this is so, increasing the amplitude of the periodic forcing to the appropriate value will generate the desired spike rate. In practice at large D, one will have to take into account the change from exponential to power-law behavior of the dependence of the mean interval on D.

Finally, for large D and small $\tilde{A}$, we show that $\partial\tilde{A}/\partial T \to -\infty$, as seen in Figs. 1(a) and 5; we can further predict the period at which the tuning curve terminates on the T-axis with infinite slope. Deriving Eq. (10) with respect to T yields

$$\frac{\partial\tilde{A}}{\partial T} = \frac{-2\theta_{n,m}D^2}{\gamma^2 T^2 R_0 \tilde{A}} \tag{11}$$

from which we can see the slope go to $-\infty$ for large D, provided $\tilde{A}$ is small. Eq. (10) in fact yields the values of T where the STC terminates on the T-axis, simply by setting $\tilde{A} = 0$. The result is $T = \theta_{n,m}/R_0$. For $D = 10^{-5}$ and $\theta_{1,1}$, we find $T = 1.46$ s, which is very close to the value that can be extrapolated from the curve in Fig. 5, as well as from the actual curves computed numerically from the FHN model in Fig. 1(a). The same holds for $D = 10^{-6}$ ($T = 19.9$) and for the 2:1 average locking pattern for $D = 10^{-}6$ ($T = 9.95$: compare Figs. 1(b) and 5). Thus, this heuristic analysis so far captures certain qualitative and quantitative features of the real tuning curves in Fig. 1, namely their lowering with increasing D at low T, and their behavior near the T-axis. However, the curves do not have the same overall shape as those in Fig. 1. One must somehow incorporate a frequency dependence into the modified Kramers rate.

4.2. Introducing frequency dependence

Fig. 6(a) plots the steady-state amplitude of the response $v(t)$ of the FHN model as a function of the period of sinusoidal forcing. The amplitude is such that the response is subthreshold for spike generation at all forcing periods. The first observation is the presence of a resonance, which shows that the 2D FHN model acts as an oscillator. The second observation is that the resonance curves, while qualitatively similar, vary quantitatively across different forcing amplitudes A. This is the hallmark of nonlinearity. For vanishing amplitude, this response of the nonlinear FHN model converges to the linear response which can be predicted simply from the linearization around its fixed point. The eigenvalues of this response are complex with negative real parts, i.e., the fixed point is a stable focus. For higher A's than those used in Fig. 6(a), spiking would occur, and the response function would exhibit a large sharp excursion over the range of suprathreshold periods.

This resonance curve underlies to a great extent the difference between the tuning curves in Fig. 1(a) and those in Fig. 5. The latter had been derived under the assumption that all forcing periods have similar effects, while it is clear that the "distance-to-threshold" decreases as periods approach the resonance. This is the basic reason for the appearance of the deterministic 1:1 curve in Fig. 1; its minimum occurs at a period close to that for which the maximal response occurs in Fig. 6(a) (even though in Fig. 6(a) the response is still subthreshold). At smaller periods, two effects conspire to raise the threshold: the decrease of the subthreshold response, but also the refractory period which mimicks an increased distance to threshold between spikes. This refractory period is increasingly important the smaller the forcing period.

We can use the resonance curves to design a heuristic correction factor for the "flat response" STCs found in the previous section. There we assumed an approximate correction to the effective potential when forcing is present, $\gamma\tilde{A}(T, D)$. To obtain a flat response when in fact the amplitude follows the resonance curve, we must "undo" the effect of this resonance by multiplying the flat response STCs by

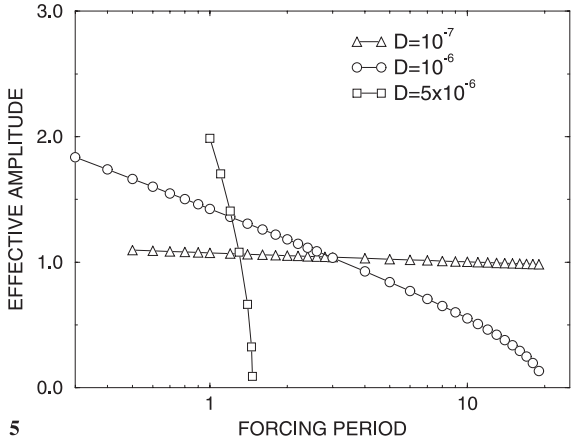

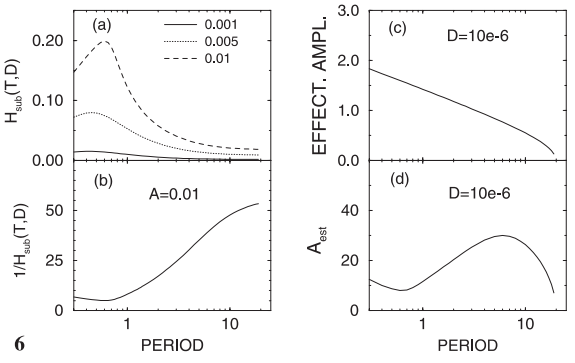

Fig. 5. Stochastic tuning curves without filtering. These curves of effective amplitude $\tilde{A}$ versus T are numerically determined based on the assumption that the mean firing rate (l.h.s. of Eq. (6)) is independent of T. For a given D, a stochastic tuning curve is obtained by numerically solving Eq. (6) for the effective amplitude $\tilde{A}$ producing 1:1 firing on average for each forcing period T.

Fig. 6. Transformation of stochastic tuning curves by the subthreshold frequency response $H_{\text{sub}}(T,D)$ of the FHN model. (a) Amplitude $H_{\text{sub}}(T,D)$ of the steady-state subthreshold membrane voltage oscillation for a fixed A in Eq. (12), as a function of forcing period T. Three curves are shown corresponding to different values of A. (b) The inverse $H_{\text{sub}}^{-1}(T,D)$ of the response for forcing amplitude $A = 0.01$ shown in (a) is plotted as a function of T. This inverse acts as a corrective filter for the stochastic tuning curves (Fig. 5) which were based on the assumption of a frequency-independent response function. (c) Stochastic tuning curve for $D = 10^{-6}$ (from Fig. 5). (d) Filtered stochastic tuning curve for $D = 10^{-6}$ obtained by multiplication of the curve in (c) by the corrective filter in (b). The resulting estimated forcing amplitude A_{est} in Eq. (1) is unnormalized.

the inverse of the resonance curve. In other words, if we call $H_{\text{sub}}(T,D)$ the frequency response function which multiplies a given input amplitude A to produce the corresponding subthreshold voltage amplitude $\tilde{A}$, then we have

$$\tilde{A}(T,D) = H_{\text{sub}}(T,D)A(T,D). \tag{12}$$

We can go from the flat response amplitude $\tilde{A}$ to an estimate $A_{\text{est}}(T,D)$ of the actual values $A(T,D)$ in Fig. 1 by simply inverting this relation, i.e., $H_{\text{sub}}^{-1}(T,D)\tilde{A}(T,D) = A_{\text{est}}(T,D)$. There is some arbitrariness as to which resonance curve to use for this purpose, and for the normalization factor as well. Our goal is not to obtain a quantitatively accurate model for the real STCs of Fig. 1, but rather a qualitative one. We simply want an approximation to the numerically determined tuning curves of the FHN model.

We choose the resonance curve corresponding to a relatively high (though subthreshold for all T) amplitude in Eq. (1), namely $A = 0.01$ (Fig. 6(a)). The inverse of this curve is shown in Fig. 6(b). Applying this inverse to the STC in Fig. 6(c) produces that in Fig. 6(d). The effect of H_{sub}^{-1} on all the STCs of Fig. 5 is shown in Fig. 7. The similarity of the resulting estimated STCs with the actual ones in Fig. 1(a) is high for $T > 1$, although there are definite quantitative differences. We note that multiplication of the STCs by $H_{\text{sub}}^{-1}(T,D)$ as in Fig. 6(b) does not alter the qualitative behavior of the STCs when they reach the T-axis (for those that do); they still do so with an infinite slope. Although it is difficult to estimate this numerically, the STCs in Fig. 1 that reach the T-axis do not seem to do so with such a slope, although the slope is large.

The curves of Fig. 7 exhibit the proper qualitative behavior for $T > 1$. While the curves have the correct upward trend as T decreases below 1, the procedure still underestimates the actual 1:1 firing thresholds. This is because, while the adiabatic theory is partially corrected for the frequency response of the two-dimensional resonant behavior of the FHN system, it still does not take the relative refractory period into account. The effect of this period is to increase the average 1:1 amplitude threshold further. As this period is more important the higher the forcing frequency, the discrepancy between the 1:1 curve predicted from our heuristic theory and the actual one worsens with increasing frequency. Although the response function H_{sub} provides less accurate information at high frequency on the 1:1 thresholds, it nevertheless adequately orders the curves, since those corresponding to higher D have a higher threshold.

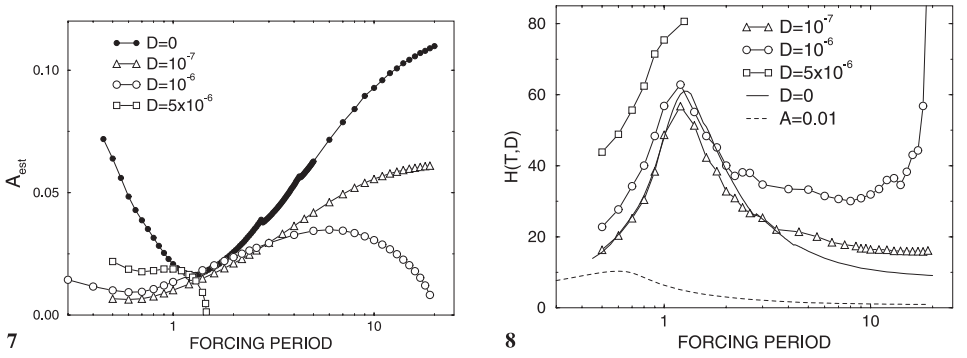

Fig. 7. Stochastic tuning curves of Fig. 5 after the filtering described in Fig. 6. The theory now assumes that the mean firing rate (l.h.s. of Eq. (6)) depends on T as well as A and D. Each curve is obtained by multiplying the corresponding curve for $D > 0$ in Fig. 5 by the same correction filter in Fig. 6(b), estimated for $A = 0.01$. The $D = 0$ 1:1 curve from Fig. 1(a) is shown for comparison. The resulting curves for $D > 0$ have been normalized by the same factor. This factor is chosen to make the curve for $D = 10^{-7}$ at $T = 19$ coincide with the numerical simulation in Fig. 1(a) for $D = 10^{-7}$ and $T = 19$. This is because the match to the adiabatic theory should be best at long periods and low noise.

Fig. 8. Value of the effective potential term $H_{1,1}(T, D)$ in Eq. (12) that satisfies the average phase-locking condition Eq. (6) when A in the model Eq. (1) is given the numerically generated values in Fig. 1(a). For comparison, the response function for the fixed amplitude $A = 0.01$ in Fig. 6(a) is also shown (dashed line), as well as the inverse of the deterministic 1:1 curve from Fig. 1(a) (solid line). The curves for $D = 10^{-6}$ and 5×10^{-6} are seen to diverge for $T = 20$ and $T = 1.46$, respectively, which are the same values at which the corresponding STCs in Fig. 1(a) reach the T-axis (i.e., at which noise alone already produces one spike per cycle on average).

5. Theory of STCs: effective potential

In this section, we address a different aspect of the problem of finding a heuristic description of FHN in terms of a one-dimensional model. The goal now is to actually estimate a function $H(T, D)$ which will satisfy the locking condition Eq. (6) given the real STCs $A(T, D)$ in Fig. 1, where A is the value in Eq. (1). We now write

$$\frac{\theta_{1,1}}{T} = R_0 I_0 \left[\frac{\gamma A(T, D) H_{1,1}(T, D)}{D} \right]. \tag{13}$$

For a given period T, noise intensity D, and corresponding threshold amplitude $A(T, D)$ in the FHN model (numerically determined and shown in Fig. 1(a)), the value of H which solves Eq. (12) can be determined using again a Newton root finding method. For simplicity we can also set $\gamma = 1$. For simplicity also, we can directly estimate H by dividing, for each D, the effective "flat response" STCs, $\tilde{A}(T, D)$ in Fig. 5, by the corresponding STCs in Fig. 1(a). Thus we do not actually have to redo the root finding calculations. The resulting curves $H_{1,1}(T, D)$ are plotted for three different D values in Fig. 8.

We find that this effective potential factor $H_{1,1}$ depends significantly on both T and D. Its magnitude can be interpreted as the propensity to generate spikes for given T and D (all other FHN parameters being fixed; of course H depends on them as well). For low D, the shape of $H_{1,1}$ seems to approach the inverse of the deterministic 1:1 curve. This is not surprising given that the same holds for the tuning curves themselves in Fig. 1(a). For low D, the $H_{1,1}$ curves are also similar to the subthreshold response curves in Fig. 6(a). However, they are more sharply peaked near $T = 1$. They also differ strongly at large T when $D \geqslant 10^{-6}$, where divergent behavior is now seen. The divergences occur at T values at which the stochastic tuning curves in Fig. 1(a) cross the axis, i.e., where a zero-amplitude forcing $A = 0$ is required to get 1:1 average locking. This divergence probably accounts for the fact that the STCs in Fig. 1(a) which reach the T-axis do so with finite negative slope, contrary to those in Fig. 5.

The low and high D curves in Fig. 8 also qualitatively differ more among each other than those in Fig. 6(a). The reason for this is that $H_{1,1}(T, D)$ carries information about the actual spiking dynamics, which is more than what is contained in the subthreshold voltage response H_{sub} at one amplitude, such as at $A = 0.01$ as we have used in Section 6. Thus, $H_{1,1}$ is more directly relevant to understanding the tuning properties for various averaged locking ratios, especially at higher frequencies, in comparison to H_{sub}

which accounts less successfully for observed tuning curve shapes (see Fig. 7). In fact, for $T < 1$, $H_{1,1}$ decreases faster than the subthreshold response function, as a consequence of two effects we have already discussed: for a fixed A, the subthreshold amplitude decreases at higher frequencies (Fig. 6(a)), and the refractory period is increasingly important at low T. In our approach, both effects at higher frequencies increase the effective barrier height ($H(T,D)$ is small), and consequently, larger amplitudes $A(T,D)$ are needed for average 1:1 firing.

These $H_{1,1}(T,D)$ functions could be incorporated into a theoretical framework for computing other aspects of the neurons response, such as those in the context of SR. It is not yet known how to derive these H from first principles, nor what the limitations of this ad hoc modified Kramers approach are. In the next section, we focus on another kind of tuning curve which describes other properties of the system.

6. Phase-locking in the D–T plane

Conventional studies of periodically driven oscillators involve analyzing the phase-locking patterns as a function of the parameters of the driving force, namely the amplitude and the period [14]. This is the approach used up to here in our paper. However, noise is also a driving parameter, and one can study phase-locking as a function of D as well as A and T. This is illustrated in Fig. 9 where curves with constant mean locking ratios are represented in the D–T plane. For a given fixed A, we find for each T the value of D producing 1:1 firing on average. The resulting stochastic phase-locking curves (see [12] for more details) are monotonic at small A, such as $A = 0.015$. For decreasing A, the curves converge to the top curve obtained for $A = 0$. This latter spontaneous firing curve plots, for each D, the mean interval between successive noise-induced firings; this mean interval is plotted using the same scale as that for the forcing period. One thus sees in this way that the noise intensity producing one spike per forcing period on average for small A is close to that which produces, on average, the same number of spikes per second when $A = 0$.

For higher A, phase-locking curves may be non-monotonic. They may even drop to zero over the range of forcing periods for which spikes occur even for $D = 0$, i.e., for suprathreshold forcing. One may call such periods the "best" periods for the cell, since from this D–T standpoint they also have the lowest threshold. In a recent study [12], we have shown that this similarity between stochastic phase-locking curves at lower amplitudes and the spontaneous firing curves is also seen when one plots the value of D maximizing the power spectral density of the spike train at the forcing frequency. We have found similar behavior for other statistics used in the SR literature. In fact, the similarity to the spontaneous curve is seen for mid-to-high frequencies, i.e., those commensurate with other (inverse) time scales in the FHN dynamics. For slower signals, the noise value optimizing these statistics becomes independent of frequency.

One can also study these issues in terms of the linearization of the time-dependent firing probability (see [12] and references therein), and also by phase synchronization (similar to phase-locking) [19]. It has recently been shown that higher forcing amplitudes in bistable as well as the FHN model bring in a synchronization regime [12,19,20]; at low amplitude, this synchronization disappears. Our results above on the frequency dependence of the subthreshold response imply that this synchronization depends not only on the amplitude of forcing, but frequency as well. In other words, there may be no synchronization for a slow periodic signal of a given amplitude, but increasing the frequency enhances the subthreshold response, and brings on a synchronization regime.

7. Application to electroreceptors

We present a preliminary investigation of the Fitzhugh–Nagumo model in the context of tuning and firing patterns in electroreceptors from weakly electric fish. This is meant to give a concrete example where the notions of phase-locking and tuning of noisy excitable cells may apply. We use the verb "may" purposefully, because the mechanisms that underlie phase-locking and firing in electroreceptors on interest are not known in any detail, since no intracellular recordings have yet been possible.

7.1. Tuning of T-units and P-units

It is known that in certain weakly electric fish, such as the brown ghost knife fish, there are receptors driven by high frequency ($\approx$ 600–800 Hz) quasi-sinusoidal electric fields generated by the electric organ discharge (EOD) of the same (and other) fish (see [21] for a review). The phase and amplitude modulations of this field are detected by two classes of tuberous receptors: T-units or time coders, and P-units or probability coders [22]. The T-units fire once per EOD cycle in a tighly phase-locked fashion; they code for phase shifts of the EOD. The P-units, on the other hand, fire in a stochastically phase-locked fashion, also known as "skipping": firings are phase-locked, with more phase jitter than for T-units, and a random integer number of EOD cycles are skipped between firings. These patterns are similar to those of auditory neurons [1], the behavior of which has been discussed in the context of stochastic resonance in [5]. P-units code for amplitude modulations, such as those due to various close objects that move relative to the fish.

The FHN model can in fact be put to good use here because of its simplicity, and also because it is suitably complex to produce action potentials, non-trivial and in fact realistic tuning characteristics, skipping in response to periodic input, beat patterns in response to two periodic inputs close in frequency (not shown). Many features of P-unit firing patterns in response to an unmodulated EOD are reproduced by the FHN model, with simultaneous sinusoidal and stochastic forcing [16,23]. Skipping firing patterns similar to those seen experimentally typically arise in the subthreshold regime, and at mid-to-high frequencies (and in particular, for frequencies higher than the reciprocal of the absolute refractory period). Further, increases in the forcing amplitude A produce shorter skips between successive spikes and consequently an increased mean firing rate, while maintaining the phase-locking, as observed experimentally [22]. This behavior underlies the terminology "probability coder": higher amplitudes produce a higher probability of firing. Increasing D in Eq. (3) has the same effect, although it simultaneously increases the jitter, and thus the variance of the peaks in the interspike interval histogram. Skipping is also seen with suprathreshold signals with $D > 0$. These observations make it plausible that noise, probably foremost of synaptic origin, may cause the skipped cycles.

One interesting distinction between T-units and P-units is their tuning curves. Although there is some quantitative variation across units, those for T-units are characteristically V-shaped, as in Fig. 1 for small noise levels, while that for P-units is opened, as in Fig. 1 for larger noise levels [21]. It is thus possible that different noise levels may underlie this difference in tuning characteristics. The differences in noise level may depend on synaptic properties, as well as on channel densities [24] in the receptors themselves and on the afferent fibers which synapse onto them. Interestingly, a recent theoretical study attributes tuning differences to such channel density differences, with no mention of any stochastic properties [25]. That model produces only periodic patterns, which are different from those observed experimentally. It is likely that a combination of deterministic and stochastic properties will underlie tuning curve differences; this possibility is presently under investigation. Ultimately, we will have to wait for intracellular recordings to confirm such hypotheses.

From a modeling perspective, we note that the sharp phase-locking displayed by T-units, and P-units as well, can arise from the action of noise on either subthreshold or suprathreshold periodic stimuli [16,23]. In the case of T-units, the noise intensity should be low, and the stimulus is probably suprathreshold. The synapses involved may also be very efficient rather than noisy. For P-units, the skipping patterns may arise from noise-induced firings with a subthreshold stimulus, or from random perturbation of firings from an otherwise periodic suprathreshold firing pattern. If noise is involved in skipping, it is probably stronger in, or has a stronger effect on the P-units. This is compatible with its tuning curve shape.

7.2. Response to EOD amplitude modulations

We just saw how noise may contribute to the open shape of the tuning curves of P-units. We now illustrate, using the FHN model, how this same noise can encode amplitude modulations of an otherwise subthreshold EOD carrier into the output spike pattern. We show in Fig. 10 that the model can act as a probability coder by applying a random amplitude modulation (AM) to the EOD. The equations are:

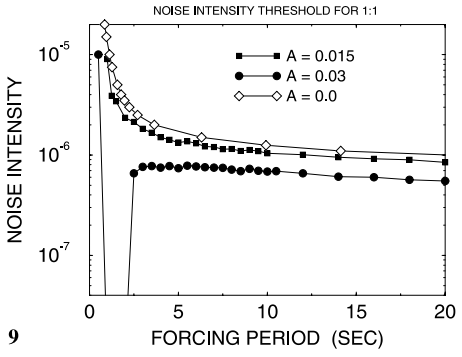

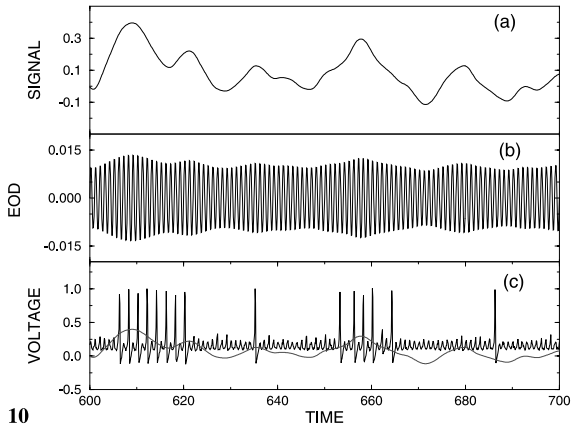

Fig. 9. Stochastic phase-locking curves in the noise intensity-forcing period subspace of parameter space. Each curve, corresponding to a given fixed forcing amplitude A in Eq. (1), is obtained by finding for each period T the intensity D that produces on average one spike per forcing cycle. The curve for $A = 0.03$ drops to the T-axis over a small range of periods, because the responses for those periods are suprathreshold in the absence of noise.

Fig. 10. Encoding random amplitude modulations in the FHN model into spike trains. (a) Time series of the random stimulus signal used to modulate the amplitude of the sinusoidal carrier known as the electric organ discharge (EOD). The modulation is produced by filtering in real time a Gaussian white noise using a lowpass filter (fourth-order pole: see Eq. (20), (b) Time series of the corresponding modulated EOD stimulus which drives the FHN model. (c) Membrane voltage of the FHN model from numerical integration of Eqs. (14)–(20) in response to the randomly modulated EOD shown in (b) as well as to an independent additive noise source as in Eq. (3). The sinusoidal carrier oscillates at 1 Hz (meant to represent ≈ 600 Hz in real time), and is subthreshold. The unmodulated EOD amplitude is 0.01, and the random Gaussian signal has zero mean and standard deviation 0.00146. The deterministic threshold for spiking at this EOD frequency is 0.0124, and thus the modulated EOD is deterministically subthreshold most of the time.

$$\epsilon \frac{dv}{dt} = v(v-a)(1-v) - \omega + A[1+s(t)]\sin\omega t + I + \eta(t), \tag{14}$$

$$\frac{d\omega}{dt} = v - d\omega - b, \tag{15}$$

$$\frac{d\eta}{dt} = -\lambda\eta + \lambda\xi_1(t), \tag{16}$$

$$\frac{ds}{dt} = z_1, \tag{17}$$

$$\frac{dz_1}{dt} = z_2, \tag{18}$$

$$\frac{dz_2}{dt} = z_3, \tag{19}$$

$$\frac{dz_3}{dt} = -4\alpha z_3 - 6\alpha^2 z_2 - 4\alpha^3 z_1 - \alpha^4 s(t) + \xi_2(t), \tag{20}$$

where the voltage dynamics are driven by two independent zero-mean noise sources. The signal $s(t)$ is obtained by lowpass filtering Gaussian white noise from a second independent source $\xi_2(t)$; the frequency response function of this filter is $H(\omega) = \alpha^4/(j\omega + \alpha)^4$. Here we use the same basic FHN parameters as in Section 2, and $\alpha = 0.5$.

In the presence of receptor noise $\eta(t)$, and in the absence of random AM's, spikes can occur which are phase-locked to the carrier. The random modulation of the carrier amplitude elicits a new pattern of spikes. The amplitude of the modulation is encoded in the instantaneous frequency of the spiking, as shown in Fig. 10: the spike rate increases when the EOD amplitude increases, and vice versa. This encoding is corrupted by the noise, yet spikes could not occur in the absence of the receptor noise. This is similar to studies of rate coding in noisy neurons [26,27], and in particular to studies of aperiodic SR [6,7].

One difference here however is that we are not directly applying the signal to the voltage dynamics: it is applied to the amplitude of a high-frequency periodic signal which drives dv/dt. Hence, although rate

coding is apparent, all firings are still precisely phase-locked to an underlying high frequency forcing. There is thus a precisely timed component to the rate coding of the AM's on a slower time scale (the ratio of the EOD frequency to the cutoff frequency for the AM's in Fig. 10 is $2\pi/\alpha = 4\pi$, which is in the physiological range). More extensive results, in particular on how the ability of the FHN system (and other more accurate models) to transmit information about EOD AM's depends on various parameters, are forthcoming.

8. Discussion

We have computed the behavior of the 1:1 and 2:1 tuning curves of the excitable Fitzhugh–Nagumo model with and without noise. In contrast to the noiseless case, noise creates a continuum of locking ratios in the subthreshold region. For mid-to-long periods, noise thus "fans out" the tuning curves into the subthreshold region. These curves can be interpreted as stochastic versions of the locking curves giving rise to deterministic phase-locking [12,14,15].

Noise effectively lowers threshold at low frequencies, such that the best frequency may no longer be the best. This opens exciting possibilities for the role of noise in shaping classic tuning curves and modifying bandwidths [3], as recent experimental findings suggest [2]. Our study also suggests that noise may underlie to a great extent the differences in tuning characteristics of intact receptors such as the T-type and P-type electroreceptors.

Our theoretical analysis, based on a heuristic modified Kramers approach, yields an reasonable description of the tuning curves for $T > 1$, i.e., for low-to-mid frequencies where relative refractory effects only weakly influence firing from one cycle to the next. For higher driving frequencies, the threshold amplitudes are also determined by the period, the noise intensity, and the frequency-dependence of the response function H, but there will be significant contributions from dynamical effects such as phase-locking and refractoriness [26]. While these effects depend on the full two-dimensional dynamics of the system, it may be possible to include them in a heuristic description of the kind proposed here, which leads to spiking response functions as in Fig. 8.

Future work should also focus on the microscopic aspect of the fluctuations [28], by either simulating the noise due to different channels using a Monte Carlo approach [24], or by using a Langevin approach [29]. In either case, one would have to make assumptions of the form of the periodic forcing at the synapse between receptor and primary afferent where the spikes are generated. Other avenues include investigating the non-trivial effects of the noise on the mean and variance of $v(t)$ (see e.g., [17]), or extending the approach in [18] to the periodic forcing case.

Explicit approximate formulae for the subthreshold response, obtained through a variety of methods such as perturbation theory, could also be included into our heuristic approach. Finally, since the FHN model has certain limitations, one may wish to modify it, or use ionic based models with or without noise [30] in order to model more specific features of the receptors of interest For example, one may wish to include a shunting-type current along with noise in the FHN model to further linearize the response of the system, which may, depending on the system, better mimick some experimentally observed interspike interval variability [31]. Adaptation may also be important to consider.

We have concentrated on the interplay between deterministic and stochastic properties of tuning curves at the level of the spike generating mechanism. While the frequency dependence of the spiking threshold is a basic property of any neuron, there are usually other filtering mechanisms specific to each sensory receptor, such as specialized transducer cells that release neurotransmitter onto the afferent nerve axon. Our work offers one approach to study the effect of changes in internal and external noise levels on tuning, especially in the presence of such filters.

Acknowledgements

This work was funded by NSERC Canada. The author thanks L. Maler, D. Chialvo and V. Apkarian for useful discussions.

References

[1] Patuzzi R, Robertson D. Tuning in the mammalian cochlea. Physiol Rev 1988;68:1009–82.
[2] Ivey C, Apkarian V, Chialvo D. Noise-induced tuning changes in mechanoreceptors. J Neurophysiol 1998;79:1879.
[3] Bolanowski Jr SJ, Gescheider GA, Verillo RT, Checkosky CM. Four channels mediate the mechanical aspects of touch. J Acoust Soc Am 1988;84:1680–94.
[4] Glass L, Graves C, Petrillo GA, Mackey MC. Unstable dynamics of a periodically driven oscillator in the presence of noise. J Theor Biol 1980;86:455–75.
[5] Longtin A, Bulsara A, Moss F. Time interval sequences in bistable systems and the noise induced transmission of information by sensory neurons. Phys Rev Lett 1991;67:656–9.
[6] Collins JJ. Stochastic resonance without tuning. Nature 1995;376:236–8.
[7] Levin JE, Miller JP. Broadband neural encoding in the cricket cercal sensory system enhanced by stochastic resonance. Nature 1996;380:165–8.
[8] Gammaitoni L, Hänggi P, Jung P, Marchesoni F. Stochastic resonance. Rev Mod Phys 1998;70:223–87.
[9] Wiesenfeld K et al. Stochastic resonance on a circle. Phys Rev Lett 1994;72:2125–2128.
[10] Jung P. Threshold devices fractal noise and neural talk. Phys Rev E 1994;50:2513–22.
[11] Collins JJ, Chow CC, Imhoff T. A periodic stochastic resonance. Phys Rev E 1995;52:R3321–4.
[12] Longtin A, Chialvo D. Stochastic and deterministic resonances in excitable systems. Phys Rev Lett 1998;82.
[13] Hochmair-Desoyer IJ, Hochmair ES, Motz H, Rattay F. A model for the electrostimulation of the nervus acusticus. Neuroscience 1984;13:553–62.
[14] Winfree AT. The geometry of biological time. New York: Springer, 1980.
[15] Chialvo V, Jalife J. Nature 1988;330:749.
[16] Longtin A. Stochastic resonance in neuron models. J Stat Phys 1993;70:309–27.
[17] Tuckwell HC, Rodriguez R. Analytical and simulation results for stochastic Fitzhugh–Nagumo neurons and neural networks. J Comput Neurosci 1998;5:91–113.
[18] Pikovsky A, Kurths J. Coherence resonance in a noise-driven excitable system. Phys Rev Lett 1997;78:775–8.
[19] Neiman A, Silchenko A, Anishchenko V, Schimansky-Geier L. Stochastic resonance: noise enhanced phase coherence. Preprint, 1998.
[20] Chialvo DR, Longtin A, Müller-Gerking J. Stochastic resonance in models of neuronal ensembles. Phys Rev E 1997;55:1798–808.
[21] Zakon H. The electroreceptive periphery. In: Bullock TH, Geiligenberg WH, editors. Electroreception. New York: Wiley, 1986:613–43.
[22] Scheich H, Bullock T, Hamstra RH Jr. Coding properties of two classes of afferent nerve fibers: high-frequency electroreceptors in the electric fish. Eigenmannia J Neurophysiol 1973;36:39–60.
[23] Longtin A, Racicot DM. Spike train patterning and forecastability. Biosystems 1997;40:111–8.
[24] DeFelice L.J., Goolsby WN. Order from randomness:spontaneous firing from stochastic properties of ion channels. Millonas MM, editor. Fluctuations and order: the new synthesis. New York: Springer, 1996:331–342.
[25] Kashimori Y, Goto M, Kambara T. Model of P- and T-electroreceptors of weakly electric fish. Biophys J 1996;70:2513–26.
[26] French AS, Holden AV, Stein RB. The estimation of the frequency response function of a mechanoreceptor. Kybernetik 1972;11:15–23.
[27] Knight B. Dynamics of encoding in a population of neurons. J Gen Physiol 1972;59:734–66.
[28] Bezrukov SM, Vodyanoy I. Noise induced enhancement of signal transduction across voltage-dependent ion channels. Nature 1995;378:362–4.
[29] Fox RF. Stochastic versions of the Hodgkin–Huxley equations. Biophys J 1997;72:2068–74.
[30] Guttman R, Feldman L, Lecar H. Squid axon membrane response to white noise stimulation. Biophys J 1974;14:941–55.
[31] Theunissen FE, Eeckman FH, Miller JP. Linearization by noise and/or additional shunting current of a modified Fitzhugh–Nagumo spiking model. In: Eeckman P, editor. Neural systems: analysis and modeling. Norwell: Kluwer, MA, 1991;77–91.